Power spectra of flow in an hourglass

C. T. Veje and P. Dimon
Center for Chaos and Turbulence Studies, The Niels Bohr Institute, Blegdamsvej 17, DK-2100 Copenhagen Ø, Denmark
(Received 12 May 1997)

We have investigated the density fluctuations of granular flow in an hourglass. When there is no counterflow of air, the flow is continuous with no visible density fluctuations. When there is a counterflow, we observe both clustering and ticking depending sensitively on the grain size and distribution, in qualitative agreement with the measurements of Wu *et al.* [Phys. Rev. Lett. **71**, 1363 (1993)]. The power spectra show structures appropriate for the different time scales. All power spectra are white at low frequencies. For certain grains there is also an apparent $1/f$ region as found earlier by Schick and Verveen [Nature (London) **251**, 599 (1974)]. However, we argue that this $1/f$ region is not genuine and can be explained by a simple stochastic model in which the clusters randomly block the measuring light source. [S1063-651X(97)01210-5]

PACS number(s): 81.05.Rm, 46.10.+z, 05.40.+j, 72.70.+m

I. INTRODUCTION

A wide variety of systems have been claimed to produce $1/f$ noise [1–7]. A classic example are the voltage fluctuations in resistors [3–5], which continue to elude explanation. We cite this particular example because it is an undisputed instance of $1/f$ noise, having been measured over no less than six decades of frequency [4]. Moreover, the presumed crossover to white noise at sufficiently low frequencies has not yet been observed.

In particular $1/f$ noise in the density fluctuations of sand flowing in an hourglass was reported by Schick and Verveen [1]. However, unlike other observations of $1/f$ noise, they observed a crossover to white noise at low frequencies. Others have also found $1/f$ density fluctuations in computer simulations of granular flow [6,7], but they only appear for special values of the flow parameters.

The Schick-Verveen (SV) experiment inspired us to construct a two-dimensional analog of an hourglass in the hope of observing and controlling the dynamics leading to the $1/f$ noise. However, we did not find any in that system [8]. We therefore repeated the SV experiment, although we were only able to reproduce their results qualitatively in certain cases. As a consequence of these measurements, however, we believe that the $1/f$ region is not genuine and we propose a simple stochastic model as a more suitable explanation.

Only a few experiments have studied flow in hourglasses other than the SV experiment. These have mainly focused on the ticking phenomenon [9] and the associated pressure variations [10]. Experiments on sand flow in long narrow tubes have also found density waves [11,12] originating from the air-grain interaction also responsible for the ticking phenomenon.

II. EXPERIMENT

A schematic of the experiment is shown in Fig. 1. The hourglass consisted of a glass tube (A) 350 mm long with a 60 mm internal diameter serving as the reservoir for a 150-mm-long tapering capillary similar to that described by Schick and Verveen. The smallest inner diameter of the capillary was 3 mm. The hourglass was supported by a frame (B) and placed on a heavy, vibration damped table. The counterflow of air was controlled by inserting a cork in the top of the tube (C). The average mass flow rate was obtained by a scale (D) (1-Hz sampling rate) placed under the outlet. A light beam from a 1-mW, 670-nm laser diode (E) was collimated to a diameter 0.2 mm and directed through the capillary 5 mm above the outlet. The detector was a photodiode with a built-in amplifier (10 kHz bandwidth) (F) also with a 0.2-mm pinhole in front of it. The signal from the photodiode was processed with a Hewlett-Packard HP3562A signal analyzer.

Table I shows the different grain types that were used. Grains A7–A30 are glass beads (droplets) in weakly polydisperse mixtures. Grains M1–M4 are mixtures of the A grains, either in equal volumes (M1,M2) or equal numbers (M3,M4) according to the mean diameter d. The grains R1 consisted of crushed glass. The volume of the glass tube was $\sim 1000\ \mathrm{cm}^3$, so with average mass flow rates varying from 0.1 to 3 g/s, typical runs lasted 10–100 min. For grains of these sizes, changes in the humidity have been found to have an important effect on the flow [12]. Thus we monitored the humidity and measurements were only made in a range of $\pm$ 3% around the mean humidity of $\sim$ 30%.

III. RESULTS

For small grains ($d < 100\ \mu$m) Wu *et al.* [9] have identified different flow regimes as a function of the orifice-grain diameter ratio D/d when there is a counterflow of air. For $D/d < 2$ they found that the flow always forms a stable arch and jams. For $2 < D/d < 12$, they observed a continuous flow. When $D/d > 12$, they found that the flow had a periodic ''ticking.'' Schick and Verveen used a polydisperse mixture $3 < D/d < 30$ (distribution unknown) of glass grains (shape unknown) with and without a counterflow of air.

Table I shows the ratio D/d for the different grain types in the present work for $D = 3$ mm. For all grain types the flow is continuous when there is no counterflow of air, i.e., the cork is out. In this case the flow in the capillary is so dense that the light beam is totally blocked.

When there is a counterflow of air, we find two main classes of behavior. For the largest grains (A30, $D/d \sim 8$) we

 © 1997 The American Physical Society

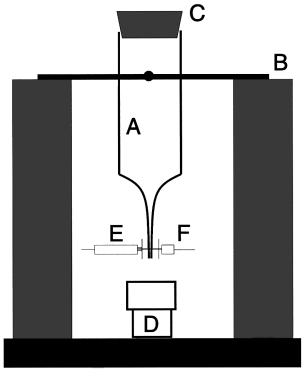

FIG. 1. Schematic of the experiment (see the text).

find that the flow is continuous since the permeability is large. For smaller grains (A7–A15, $D/d>12$) or broader mixtures (M1–M4) we find that the counterflow generates different regimes of clustering and ticking phenomena. These qualitative results are consistent with the observations of Wu *et al.* [9] insofar as we can compare experiments with somewhat different geometries and grain sizes. We do not see the regular wave patterns with constant velocity observed in some experiments [11,12] probably because our capillary has no constant diameter section.

When sand flows, it creates a pressure drop in the upper compartment and hence a pressure gradient across the capillary [9,10,12]. For small grains (A7), the pressure gradient stabilizes an air-grain interface at some point in the capillary and the grain flow pauses until the gradient has decreased sufficiently for this stationary interface to break. Then a cluster of grains falls out of the capillary, creating a new gradient, and a new interface is formed at a point higher up in the capillary, leaving the remaining grains at rest. In Fig. 2 we show the time signal recorded by the photodiode for this flow. The clusters of grains falling out are seen as bursts in the signal with a time scale of roughly 5-s duration. At a characteristic position some 10 cm above the outlet the interface cannot be sustained further due to the increasing cross section of the capillary. The whole capillary then fills once again and the entire process repeats itself. The process of refilling creates a large pressure gradient once again since a quantity of grains, corresponding to the volume of the capillary, is removed from the reservoir almost instantly. Then the grains remain stationary with a stable interface at the outlet and fill the whole capillary, blocking the beam completely. The time for this large pressure gradient to equilibrate is relatively long and can be seen in Fig. 2 as the longer pauses with a blocked beam of $\sim$ 20 s. Wu *et al.* [9] give an expression for the relaxation time τ_r associated with the ticking as $\tau_r=\eta V/\pi p\kappa R$, where η is the dynamic viscosity of air, V is the volume of the reservoir, p is the external pressure, κ is the permeability, and R is the grain radius. For $\eta=1.7\times10^{-4}$g/cm s, $V\sim1000\text{cm}^3$, $p\sim10^6$dyn/cm^2, $\kappa\sim1.2\times10^{-7}$cm^2, and $R\sim10^{-2}$ cm, we find a relaxation time $\tau_r\sim45$ s, in rough agreement with the measurements.

TABLE I. Grain types used in the experiment. We give the approximate size range and the mean diameter d. M1–M4 consist of various grain mixtures (see the text) for which D/d is computed using the size range for d.

Type	Size (μm)	d (μm)	D/d
A7	70–110	100	30
A10	100–200	180	18
A15	150–250	230	13
A30	300–400	380	8
M1	70–250		13–30
M2	70–400		8–30
M3	70–250		13–30
M4	70–400		8–30
R1	200–500	400	8

The above behavior has two characteristic time scales: the time between successive clusters falling out of the capillary and the refilling of the capillary. In Figs. 3(a)–3(d) we show the power spectra for grains A7, A10, and A15 and the rough grains R1, respectively. As shown in Fig. 3(a), the time scales for grain A7 are not periodic. For low frequencies the spectra are white. The time between clusters gives a rolloff in the spectrum after which the power spectrum $S(f)\sim f^{-2}$ due to the discontinuities in the signal. At higher frequencies the spectrum becomes nearly white again and then rolls off very rapidly due to the resolution function of the measuring system.

For the larger grains (A10–A15) the permeability is larger, which changes the dynamics. Here the grains fall out continuously from the high-density stationary region filling the capillary. This gives an interface propagating upward similar to the cluster–air-bubble interface found in long narrow tubes [11,12]. Again, when the interface reaches a characteristic point in the upper part of the capillary, refilling occurs. As before, the refilling creates a large pressure gradient and the flow pauses for a few seconds with a stationary interface at the outlet. A typical signal of this behavior is shown in Fig. 4 for the flow of grain A15. This signal is almost periodic, as can also be seen from the spectra shown in Figs. 3(b) and 3(c). There are clear peaks from the refilling of the capillary. Thus the dynamics has changed from random to nearly periodic simply by changing the size of the grains.

This qualitative behavior is in principle similar for the mixtures M1–M4 whose spectra are shown in Figs. 5(a)–5(d). In Fig. 5(a) we show the spectrum for M1. It is simply grain A7 mixed in equal volumes with the larger grains A10 and A15. Comparing this with Fig. 3(a), for grain A7 alone, we see that the addition of larger grains has resulted in a broad peak at low frequencies. Adding even larger grains (A30) produces the spectrum for M2 shown in Fig. 5(b).

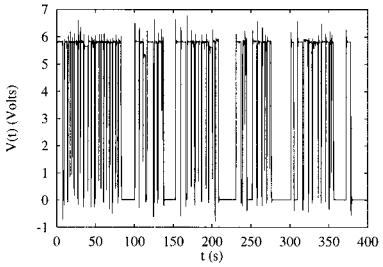

FIG. 2. Time signal with the fine grains A7. The output is $\sim$0 V for a blocked beam.

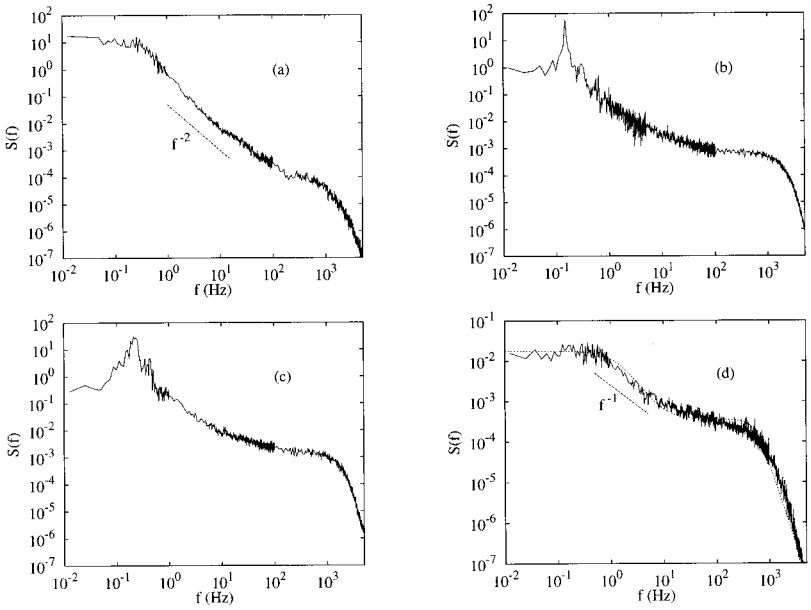

FIG. 3. Power spectra for the A-type grains: (a) A7, (b) A10, (c) A15, and (d) R1. The dotted line in (d) is a fit using the random switching model (see Sec. IV). The dashed lines are shown for reference.

Now there is a clear peak and possibly even its first harmonic. Thus, by adding larger grains and therefore increasing the permeability, the dynamics has become more periodic. This is consistent with the observations of the A-type grains.

Since the mixtures M1 and M2 consist of equal volumes of A-type grains, the smaller grains far outnumber the larger ones. If we do the mixing in equal numbers, we form the mixtures M3 and M4 whose spectra are shown in Figs. 5(c) and 5(d), respectively. The spectrum for M3, where the A15 grains constitute $\sim$65% of the total grain volume, looks very similar to the spectrum of A15 grains in Fig. 3(c). This comparison shows that adding a small amount of smaller grains to A15 results in no apparent change in the dynamics. For the mixture M4, where $\sim$75% of the grain volume is A30 grains, we see noticeable changes in the dynamics. Recall that the flow of A30 grains alone was continuous. By adding a small amount of smaller grains the permeability is decreased since the small grains block the interstices. The lower permeability is apparently sufficient to produce ticking.

For the rough sand R1 the dynamics is found to be significantly different. This sand consists of too large a fraction of large grains (80%$>$350 μm) for ticking to occur, i.e., the permeability is too large. However, the rough surface of the grains produces enough friction with other grains, the capillary wall, and air for clustering to take place. We observe voids, which are regions of dilute flow, created near the outlet and they propagate 1–2 cm up through the capillary before decaying. This behavior is most similar to that described by Schick and Verveen.

In Fig. 6 we show the time signal for the R1 grains. The passing of the voids is seen as noise bursts separated by regions where the beam is totally blocked. The spectrum is shown in Fig. 3(d). The characteristic length of the voids corresponds to $\sim$1 Hz. The spectrum then falls off to the noise level and finally rolls off due to the resolution function. Note that it is possible to fit about a decade of the spectrum to the form $S(f)\sim f^{-\alpha}$ with $\alpha\sim 1$. We believe that the apparent decade of $1/f$ noise in the SV experiment is similar to that found here.

IV. RANDOM SWITCHING MODEL

Upon closer inspection of the time signal in Fig. 6, we realize that a rather simple model might produce the shape of the power spectrum shown in Fig. 3(d). We model the raw signal $v(t)$ as the product of the signal $v_2(t)$ corresponding to dilute flow in the voids and a signal $v_1(t)$ representing the clusters that switch the dilute flow on and off, i.e., $v(t)=v_1(t)v_2(t)$. This qualitatively describes the signal shown in Fig. 6. The autocorrelation function of $v(t)$ is $C_v(\tau)=\overline{v(t+\tau)v(t)}$. If $v_1(t)$ and $v_2(t)$ are uncorrelated, then $C_v(\tau)=C_1(\tau)C_2(\tau)$, where $C_{1,2}(\tau)$ is the autocorrelation function of $v_{1,2}$. The power spectrum is $S(\omega)=\int C(\tau)e^{i\omega\tau}d\tau$ $(\omega=2\pi f)$ and using the convolution theorem we find that

$$S_v(\omega)=\frac{1}{2\pi}\int S_1(\omega')S_2(\omega-\omega')d\omega'. \tag{1}$$

Thus we need only to determine the power spectra of v_1 and v_2 separately.

Now let us consider again the time signal in Fig. 6. We will specifically model v_1 (the switching signal) by a random sequence of square pulses that are ''on'' for a mean time σ

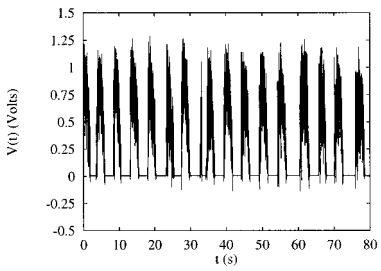

FIG. 4. Time signal with grains A15. The output is $\sim$0 V for a blocked beam.

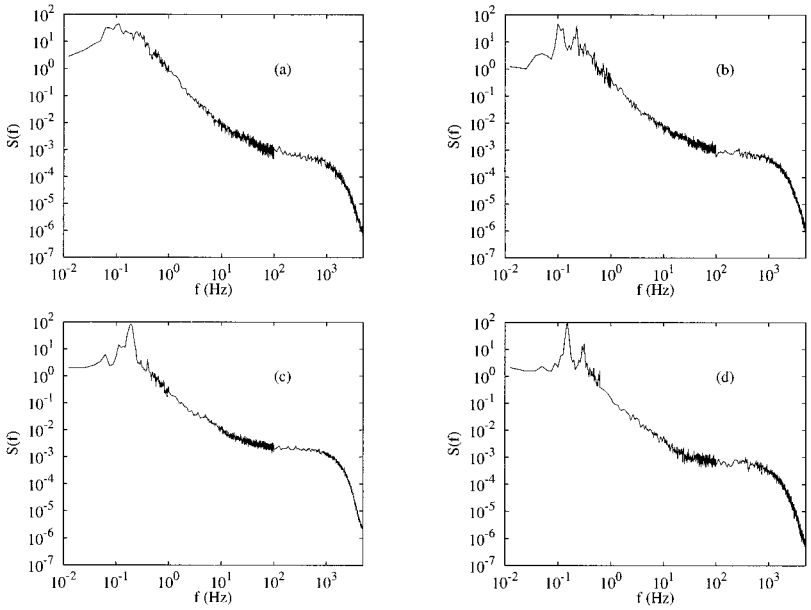

FIG. 5. Power spectra for the M-type mixtures: (a) M1, (b) M2, (c) M3, and (d) M4.

and ''off'' for a mean time μ. The power spectrum of such a random sequence of square pulses has been calculated by Machlup [13] to be

$$S_1(\omega)=2\pi\sigma^2\nu^2\delta(\omega)+\frac{2\nu T^2}{1+\omega^2T^2}, \tag{2}$$

where $\nu=1/(\sigma+\mu)$ is the pulse rate and $1/T=1/\sigma+1/\mu$. We will model the dilute flow within the voids as Gaussian white noise $\eta(t)$ with a finite mean, i.e., $\langle\eta(t)\rangle=\eta_0$ and $\langle\eta(t)\,\eta(t')\rangle=\eta_0^2+2\Gamma\,\delta(t-t')$. Its power spectrum is then just

$$S_2(\omega)=2\pi\eta_0^2\delta(\omega)+2\Gamma. \tag{3}$$

Substituting Eqs. (2) and (3) into Eq. (1), we find

$$S_v(\omega)=A\left[1+\frac{B}{1+\omega^2T^2}\right], \tag{4}$$

where $A=2\nu\sigma\Gamma$, $B=\nu\mu T\eta_0^2/\Gamma$, and we have omitted the δ-function term.

The measured signal $V_M(t)$ is the convolution of the signal $v(t)$ with the resolution function $R(t)$, i.e., $V_M(t)=\int v(t')R(t-t')dt'$. Using the convolution theorem again, we can write the measured power spectrum as

$$S_M(\omega)=S_v(\omega)S_R(\omega). \tag{5}$$

Empirically, we will take the resolution function to be $S_R(\omega)=1/(1+\omega^4T_R^4)$ with $T_R=0.0015$ s. We can estimate the parameters in Eq. (2) from the signal in Fig. 6. We take $\nu=0.5\text{s}^{-1}$ and $\sigma=0.3$ s so that $T=0.12$ s. The only unknown parameters are then η_0^2/Γ and the overall amplitude A. A fit to Eq. (5) is shown as the dotted line in Fig. 3(d).

As already noted, there is an apparent decade of $1/f$ noise as the spectrum crosses over from the spectrum $S_1(f)$ to $S_2(f)$. The measured spectrum, however, does not then become white as in the model, but perhaps $v_2(t)$ does not actually have a white spectrum as we have assumed. (The model is meant to be more pedagogical than quantitative, so we have presented it in its simplest form.) We believe that the SV data have the same qualitative shape as that shown in Fig. 3(d), that is, they did not observe genuine $1/f$ noise but merely a crossover between time scales.

It may be, however, that ''real'' $1/f$ noise can be found if there is a large number of switching time constants covering a sufficiently large range of time scales. The kind of discrete switching described here has, in fact, been observed by Ralls *et al.* [14] in very small metal-oxide-semiconductor field-effect transistors and they have suggested that this process may indeed lead to $1/f$ noise. The random switching model can, of course, be generalized to include many uncorrelated switching functions v_j, $j=1,N$. In this case, $C(\tau)=\Pi_{j=1}^{N}C_j(\tau)$ and the power spectrum can be written in the form

$$S_v(\omega)=\frac{1}{(2\pi)^{N-1}}\int d\omega_1 d\omega_2\cdots d\omega_N \times\delta\left(\omega-\sum_{j=1}^{N}\omega_j\right)\prod_{j=1}^{N}S_j(\omega_j). \tag{6}$$

If the spectra $S_j(\omega)$ all have a form similar to Eq. (2), then $S_v(\omega)$ will consist of sums and convolutions of Lorentzian functions. It is well known that a superposition of Lorentzians can yield $1/f$ noise, i.e., $S(\omega)\sim\int d\tau D(\tau)/(1+\omega^2\tau^2)\sim 1/\omega$ if the distribution of time constants $D(\tau)\sim 1/\tau$ over a sufficiently large range of τ [15].

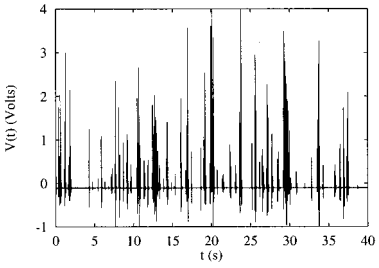

FIG. 6. Time signal for the rough sand R1. The output is ~ 0 V for a blocked beam.

ACKNOWLEDGMENTS

It is a pleasure to thank R. B. Behringer, A. M. Hansen, H. J. Herrmann, K. J. Måløy, E. Nowak, and T. Raafat for many interesting discussions. The authors would also like to thank the Danish Science Foundation (Statens Naturvidenskabelige Forskningsråd) and Novos Fond for support.

[1] K. L. Schick and A. A. Verveen, Nature (London) **251**, 599 (1974).
[2] W. H. Press, Comm. Ast. **7**, 103 (1978).
[3] P. Dutta and P. M. Horn, Rev. Mod. Phys. **53**, 497 (1981).
[4] B. Pellegrini, R. Saletti, P. Terreni, and M. Prudenziati, Phys. Rev. B **27**, 1233 (1983).
[5] M. B. Weissman, Rev. Mod. Phys. **60**, 537 (1988).
[6] G. H. Ristow and H. J. Herrmann, Phys. Rev. E **50**, R5 (1994).
[7] G. Peng and H. J. Herrmann, Phys. Rev. E **49**, 1796 (1994); **51**, 1745 (1995).
[8] C. T. Veje and P. Dimon, Phys. Rev. E **54**, 4329 (1996).
[9] X. Wu, K. J. Måløy, A. Hansen, M. Ammi, and D. Bideau, Phys. Rev. Lett. **71**, 1363 (1993).
[10] T. Le Pennec, K. J. Måløy, A. Hansen, M. Ammi, D. Bideau, and X. Wu, Phys. Rev. E **53**, 2257 (1996).
[11] T. Pöschel, J. Phys. I **4**, 499 (1994).
[12] T. Raafat, J. P. Hulin, and H. J. Herrmann, Phys. Rev. E **53**, 4345 (1996); Phys. Fluids (to be published).
[13] S. Machlup, J. Appl. Phys. **25**, 341 (1954).
[14] K. S. Ralls, W. J. Skocpol, L. D. Jackel, R. E. Howard, L. A. Fetter, R. W. Epworth, and D. M. Tennant, Phys. Rev. Lett. **52**, 228 (1984).
[15] J. Bernamont, Proc. Phys. Soc. London **49**, 138 (1937); F. K. DuPré, Phys. Rev. **78**, 615 (1950); A. van der Ziel, Physica (Amsterdam) **16**, 359 (1950).